

AD-A255 902



AEROSPACE REPORT NO.
TR-0091(6925-08)-4

Determining Optimum C-Field Settings that Minimize Output Frequency Variations in Cesium Atomic Frequency Standards

Prepared by

S. K. KARUZA, W. A. JOHNSON, and F. J. VOIT
Communications Systems Subdivision
and
J. P. Hurrell
Electronics Technology Center

15 December 1991

Prepared for

SPACE AND MISSILE SYSTEMS CENTER
(formerly Space Systems Division)
AIR FORCE MATERIEL COMMAND
Los Angeles Air Force Base
P. O. Box 92960
Los Angeles, CA 90009-2960

Engineering and Technology Group

THE AEROSPACE CORPORATION
El Segundo, California

APPROVED FOR PUBLIC RELEASE:
DISTRIBUTION UNLIMITED

DTIC
ELECTE
SEP 29 1992
S A D

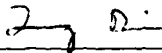
92-26084

92 9 28 113

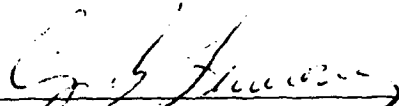
This report was submitted by The Aerospace Corporation, El Segundo, CA 90245-4691, under Contract No. F04701-88-C-0089 with the Space and Missile Systems Center, P. O. Box 92960, Los Angeles, CA 90009-2960. It was reviewed and approved for The Aerospace Corporation by J. M. Straus, Principal Director, Communications Systems Subdivision. Lt. Tenerowicz was the project officer for the Mission-Oriented Investigation and Experimentation (MOIE) program.

This report has been reviewed by the Public Affairs Office (PAS) and is releasable to the National Technical Information Service (NTIS). At NTIS, it will be available to the general public, including foreign nationals.

This technical report has been reviewed and is approved for publication. Publication of this report does not constitute Air Force approval of the report's findings or conclusions. It is published only for the exchange and stimulation of ideas.



QUANG BUI, Lt, USAF
MOIE Program Manager



CYNTHIA B. TENEROWICZ, 1Lt, USAF
Payload Development Engineer
GPS Space Segment

UNCLASSIFIED

SECURITY CLASSIFICATION OF THIS PAGE

REPORT DOCUMENTATION PAGE

1a. REPORT SECURITY CLASSIFICATION Unclassified			1b. RESTRICTIVE MARKINGS		
2a. SECURITY CLASSIFICATION AUTHORITY			3. DISTRIBUTION/AVAILABILITY OF REPORT Approved for public release; distribution unlimited		
2b. DECLASSIFICATION/DOWNGRADING SCHEDULE					
4. PERFORMING ORGANIZATION REPORT NUMBER(S) TR-0091(6925-08)-4			5. MONITORING ORGANIZATION REPORT NUMBER(S) SMC-TR-92-49		
6a. NAME OF PERFORMING ORGANIZATION The Aerospace Corporation Technology Operations		6b. OFFICE SYMBOL (If applicable)	7a. NAME OF MONITORING ORGANIZATION Space and Missile Systems Center		
6c. ADDRESS (City, State, and ZIP Code) El Segundo, CA 90245-4691			7b. ADDRESS (City, State, and ZIP Code) Los Angeles Air Force Base Los Angeles, CA 90009-2960		
8a. NAME OF FUNDING/SPONSORING ORGANIZATION		8b. OFFICE SYMBOL (If applicable)	9. PROCUREMENT INSTRUMENT IDENTIFICATION NUMBER F04701-88-C-0089		
8c. ADDRESS (City, State, and ZIP Code)			10. SOURCE OF FUNDING NUMBERS		
			PROGRAM ELEMENT NO.	PROJECT NO.	TASK NO.
			WORK UNIT ACCESSION NO.		
11. TITLE (Include Security Classification) Determining Optimum C-Field Settings that Minimize Output Frequency Variations in Cesium Atomic Frequency Standards					
12. PERSONAL AUTHOR(S) Karuza, Sarunas K.; Johnson, Walter A.; Voit, Frank J.; and Hurrell, John P.					
13a. TYPE OF REPORT		13b. TIME COVERED FROM _____ TO _____		14. DATE OF REPORT (Year, Month, Day) 1991 December 15	
				15. PAGE COUNT 25	
16. SUPPLEMENTARY NOTATION					
17. COSATI CODES			18. SUBJECT TERMS (Continue on reverse if necessary and identify by block number)		
FIELD	GROUP	SUB-GROUP			
19. ABSTRACT (Continue on reverse if necessary and identify by block number) <p>De Marchi at the National Institute of Standards and Technology (NIST) performed an experiment on Hewlett-Packard cesium (Cs) frequency standards, in which he showed that there exist optimum values of the C-field that make the output frequency insensitive to variations in microwave power. Moreover, and most important, De Marchi demonstrated that the long-term stability of the Cs standard was improved at these optimum values of the C-field.</p> <p>To see if these results could be obtained with standards made by different manufacturers and having different modulation schemes and Cs tube designs, we performed a similar study using a completely automated measurement system on four Cs standards made by two other manufacturers. Our results, similar to those of De Marchi, showed that there are similar optimum C-field settings in these standards; furthermore, they showed that it may be more important to tune the microwave cavity precisely to the center Cs resonance frequency (f_0) than it is to set the C-field at an optimum value. The best procedure, of course, is to do both, i.e., tune the cavity to the Cs resonance frequency as well as set an optimum C-field.</p>					
20. DISTRIBUTION/AVAILABILITY OF ABSTRACT <input checked="" type="checkbox"/> UNCLASSIFIED/UNLIMITED <input type="checkbox"/> SAME AS RPT. <input type="checkbox"/> DTIC USERS				21. ABSTRACT SECURITY CLASSIFICATION Unclassified	
22a. NAME OF RESPONSIBLE INDIVIDUAL			22b. TELEPHONE (Include Area Code)		22c. OFFICE SYMBOL

PREFACE

The authors are grateful to David W. Allan and Andrea De Marchi of the National Institute of Standards and Technology, and to Ronald L. Beard and Frederick Danzy of the Naval Research Laboratory, for their helpful and stimulating discussions and assistance in supplying some of the hardware and long-term frequency-stability measurements.

Accession For	
NTIS CRA&I	<input checked="" type="checkbox"/>
DTIC TAB	<input type="checkbox"/>
Unannounced	<input type="checkbox"/>
Justification	
By	
Distribution /	
Availability Codes	
Dist	Availability Codes Special
A-1	

DTIC QUALITY INSPECTED 3

CONTENTS

INTRODUCTION	7
MEASUREMENT SYSTEM.....	9
MEASUREMENT RESULTS.....	13
INACCURACIES IN THE MEASUREMENT SYSTEM	19
CONCLUSIONS.....	23
REFERENCES	25

FIGURES

1. The difference in the average frequencies for two power levels (P_0 and $P_0 + 1$ dB) as a function of C-field in in HP 1653 Cs frequency standard.	8
2. Block diagram of the C-field measurement system for a Cs frequency standard	10
3. Circuit diagram of the single-mixer frequency measurement system used to determine the fractional frequency changes at different C-field settings	10
4. Block diagram of the Cs beam tube microwave cavity measurement system	11
5. A plot of the difference of the average frequencies as a function of the C-field of the first Cs frequency standard for three microwave power changes (-1, +1, and +3 dB) with respect to the optimum power level, P_0	14
6. Average of final data of the first Cs frequency standard on the difference of the average frequencies as a function of C-field for a microwave power change of +1 dB above the optimum power level, P_0	14
7. The measured Allan standard deviation of the first Cs frequency standard at the non-optimum (power-sensitive) Zeeman frequency setting of 44 kHz	15
8. The measured Allan standard deviation of the first Cs Frequency standard at the optimum (power-insensitive) Zeeman frequency setting of 37 kHz.....	15
9. Plot of the microwave cavity return loss of the second Cs frequency standard tuned to a Cs resonance frequency	16
10. A plot of the difference of the average frequencies as a function of the C-field of the second Cs frequency standard for three microwave-cavity tuned frequencies (f_0 and ± 12 MHz) for a microwave power change of +3 dB above the optimum power level, P_0	16
11. A plot of the difference of the average frequencies as a function of the C-field of the third Cs frequency standard for three microwave-cavity tuned frequencies (f_0 and ± 40 MHz) for a microwave power change of +1 dB above the optimum power level, P_0	18
12. A plot of the difference of the average frequencies as a function of the C-field of the fourth Cs frequency standard for three microwave-cavity tuned frequencies (f_0 and ± 20 MHz) for a microwave power change of +3 dB above the optimum power level, P_0	18
13. A plot of power measurements made during the C-field experiment.....	20
14. A plot of the calculated contribution of microwave power changes to the Allan standard deviation for Cesium Clock No. 1	21

TABLE

1. Measurement Data	20
---------------------------	----

INTRODUCTION

De Marchi has presented experimental evidence^[1,2] on five Hewlett-Packard (HP) model 1650 dual-beam cesium (Cs) frequency standards that confirms that Rabi pulling and cavity pulling are the major transducing effects that turn microwave power variations into frequency changes. It was found that there are C-field values for which the output frequency of the Cs standards is insensitive to changes in microwave power (P).

In Fig. 1 is a plot, calculated from De Marchi's data^[1], of the fractional frequency change for a +1-dB change in microwave power as a function of the Zeeman frequency (f_z), after the Cs beam tube's microwave cavity is carefully tuned by maximizing the Cs beam current. It can be seen that there are four Zeeman frequencies (corresponding to four C-field settings) where the change in frequency will be zero for a change in microwave power of +1 dB. The peak-to-peak change in fractional frequency over the range of C-fields plotted is about 5×10^{-12} . The Zeeman frequency difference between adjacent C-field zero crossings of the Rabi-pulling curve is about 8.9 kHz. The frequency sensitivity at the 39-kHz zero crossing is $0.62 \times 10^{-12}/\text{kHz}$ for a +1-dB microwave power change. De Marchi^[1] showed that long-term frequency stability was improved by about an order of magnitude if the Zeeman frequency was set at 39 kHz (optimum frequency), rather than at a nonoptimum Zeeman frequency of 53 kHz.

De Marchi stated^[1] that the results he had obtained on the HP Cs standards should be "... at least typical for all Cs standards ...". He cautioned, however, that results obtained on Cs frequency standards that used different servo-loop schemes other than sine wave or slow square-wave frequency modulation might be somewhat different. Consequently, considerable interest developed to determine if the stability of other Cs frequency standards using different modulation schemes could be improved by this technique of optimum C-field setting. Measurements similar to those of De Marchi were made in our own laboratory on four Cs standards, from two different manufacturers, that used single-beam optics and different modulation schemes. Because the measurements are very time-consuming, it was decided to automate them completely in order to maximize the data-taking time available. An additional advantage of this automation is that one never has to make and remake microwave power connections.

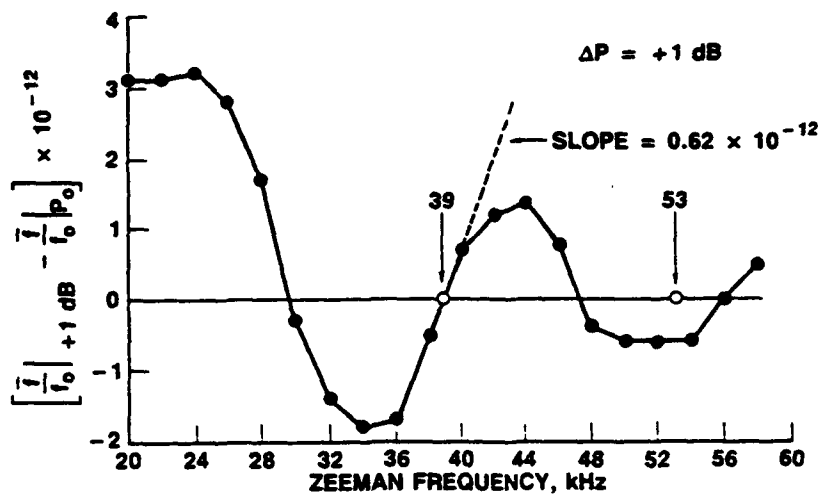


Figure 1. The difference in the average frequencies for two power levels (P_0 and $P_0 + 1 \text{ dB}$) as a function of C-field in in HP 1653 Cs frequency standard.

MEASUREMENT SYSTEM

The C-field experiment was performed in our laboratory on four Cs frequency standards. These standards were modified to allow access to the C-field coil wires and the microwave power source. Figure 2 shows the block diagram of the complete measurement system. Both of the parameters that are varied, namely the C-field current and the microwave power, are computer controlled; the current is set by a precision constant-current generator and the microwave power is changed by a calibrated PIN diode attenuator. The entire system is controlled by an HP series 300 computer, which also acquires and processes the data.

Figure 3 is a block diagram of the frequency measurement system. The frequency reference for both the Fluke synthesizer and the HP counter is an HP model 5061A-004 Cs frequency standard. Before the data are taken, the microwave cavity of the Cs tube must be tuned. Figure 4 shows the block diagram of the microwave-cavity tuning measurement system, which measures the return loss of the Cs tube's microwave cavity. The microwave tuning is adjusted to obtain a maximum return loss at the resonant frequency (f_0) of 9.192631770 GHz. The microwave power is then adjusted to maximize the output current from the beam tube. The resulting microwave power is called the optimum power (P_0).

A typical data-taking sequence consisted of the following steps:

1. Set the C-field current at some low value (typically 6 to 8 mA) and the microwave power at some value (e.g. at the optimum value P_0).
2. Measure the beat frequency over some long averaging time T (typically 7000 sec).
3. Change the microwave power level (e.g. to $P_0 + 1$ dB).
4. Measure the beat frequency over T again.
5. Increase the C-field current by some programmed amount (typically 0.5 mA).
6. Measure the beat frequency over T again.
7. Change the microwave power back to the initial value.
8. Repeat steps 2 through 7 until the final C-field current (typically 20 to 25 mA) is reached.

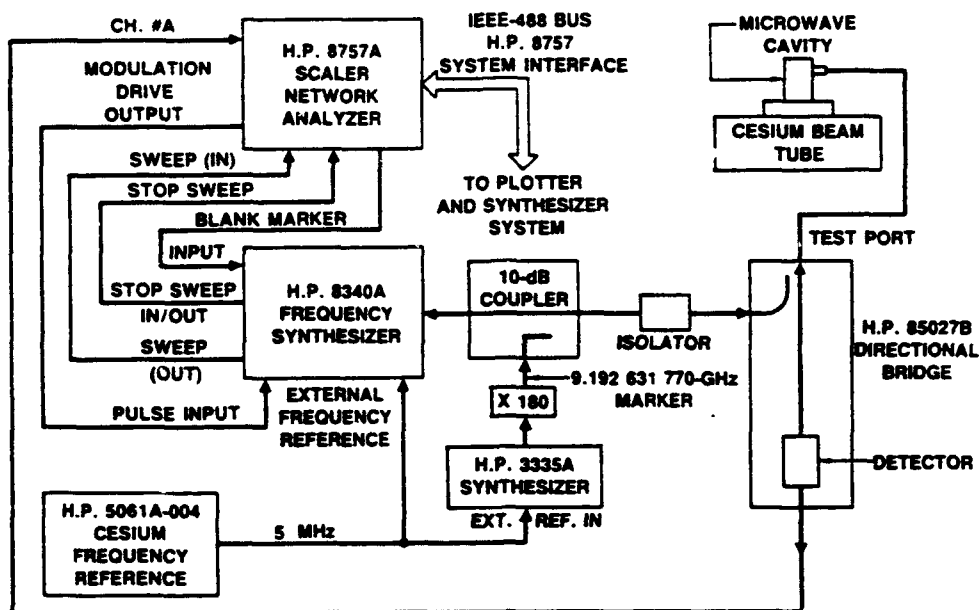


Figure 4. Block diagram of the Cs beam tube microwave cavity measurement system.

MEASUREMENT RESULTS

Figure 5 shows the results of measurements made on the first of four Cs frequency standards after the tube's microwave cavity was tuned to f_0 for changes in the microwave power level of -1, +1, and +3 dB. For the -1-dB data, each point represents the difference between two 7000-sec samples; for the +1-dB data, each point represents the difference between two 14,000-sec samples; and for the +3-dB data, each point represents the difference between two 21,000-sec samples. Each data point is calculated as the difference in output frequency between the frequency at the higher power and the lower power, both of which are normalized to the nominal output. In other words,

$$\text{ordinate} = (\bar{f}_H - \bar{f}_L)/5 \text{ MHz} \quad (1)$$

where \bar{f}_H is the average output frequency for the higher microwave power and \bar{f}_L is the average output frequency for the lower microwave power. As Fig. 5 shows, for the +1-dB and -1-dB data there is a zero crossing at about 26 kHz, but it is difficult to see if there are any other zero crossings. For the +3-dB data it is clear that there are two zero crossings, at about 25 and 37 kHz.

Because De Marchi, using the HP Cs frequency standard, had found multiple zero crossings for a +1-dB power change (Fig. 1), it was decided to spend the time to make a statistically significant measurement on this first Cs frequency standard for the same +1-dB change. Figure 6 shows the results of this measurement, with each data point representing the difference between two long samples (the error bars represent +2 standard deviations). The sample lengths varied from 30,000 to 210,000 sec. These data show distinct zero crossings at about 25 and 37 kHz, in agreement with the earlier results for the larger power change of +3 dB. Thus, by using data for the 3-dB change, it may be possible to shorten greatly the amount of time it takes to determine the location of the 1-dB zero crossing. This could reduce the data-taking time to as few as two or three days.

As Fig. 6 shows, the slope at the 37-kHz zero crossing is $0.11 \times 10^{-12}/\text{kHz}$, compared to the slope of $0.62 \times 10^{-12}/\text{kHz}$ for the HP standard (Fig. 1). Thus, for a given departure from the optimum Zeeman frequency, the frequency of the first Cs frequency standard would be from five to six times less sensitive to power changes than would be that of the HP standard.

The first Cs frequency standard was taken to the National Institute of Standards and Technology (NIST) at Boulder, Colorado, for an evaluation of the standard's long-term frequency stability at C-field settings of Zeeman frequencies of 37 kHz (optimum setting) and 44 kHz (nonoptimum setting). Figure 7 shows the Allan standard deviation of the frequency standard at 44 kHz and Fig. 8 at 37 kHz. From these results we can say only that there was no obvious improvement in the long-term frequency stability for this standard when it was set at an optimum C-field setting.

The second Cs frequency standard was also a single-beam type, with the same type of modulation scheme as the first. It was decided that on this standard we would also measure the effect of the cavity pulling on the C-field curve. The tube cavity's return loss was measured by means of the measurement system shown in Fig. 4. Tuning was accomplished by varying two tuning screws on the microwave transition piece at the input of the Cs tube. The plot of the return loss of the tuner and tube is shown in Fig. 9. Also shown are return losses for a short-circuit reference and a matched termination. The cavity was tuned first to the Cs resonance at f_0 (9.192631770 GHz). Changes in output frequency

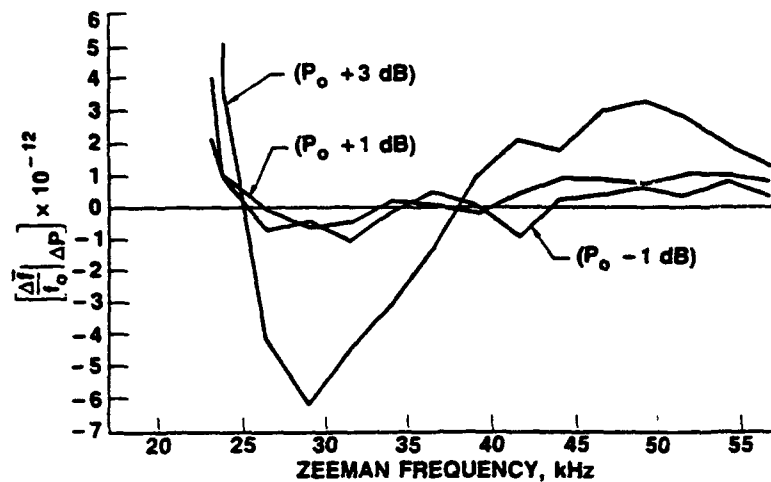


Figure 5. A plot of the difference of the average frequencies as a function of the C-field of the first Cs frequency standard for three microwave power changes (-1, +1, and +3 dB) with respect to the optimum power level, P_0 .

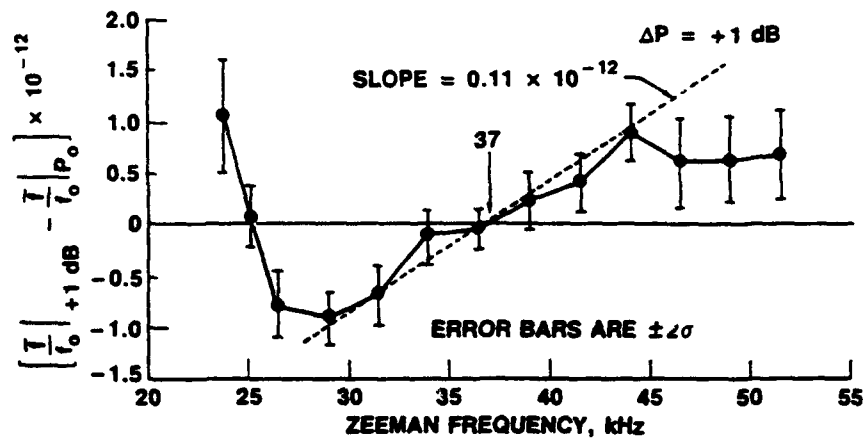


Figure 6. Average of final data of the first Cs frequency standard on the difference of the average frequencies as a function of C-field for a microwave power change of +1 dB above the optimum power level, P_0 .

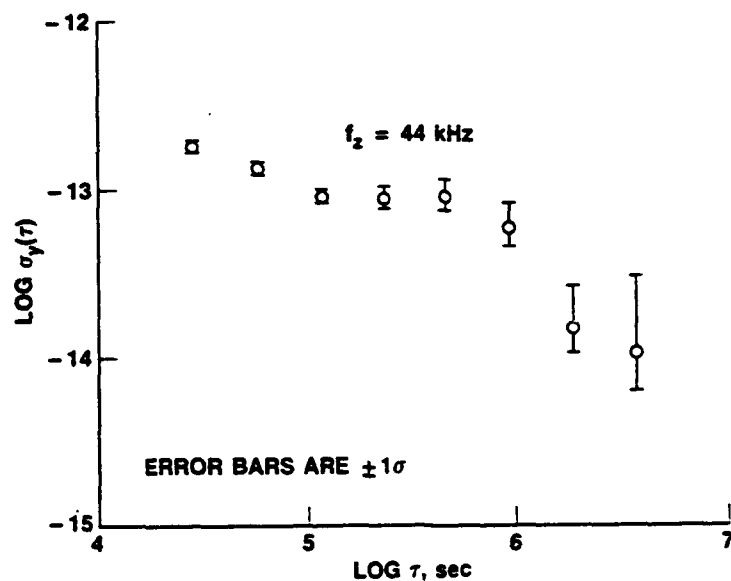


Figure 7. The measured Allan standard deviation of the first Cs frequency standard at the non-optimum (power-sensitive) Zeeman frequency setting of 44 kHz. The confidence intervals are 95%. (Data taken by NIST.)

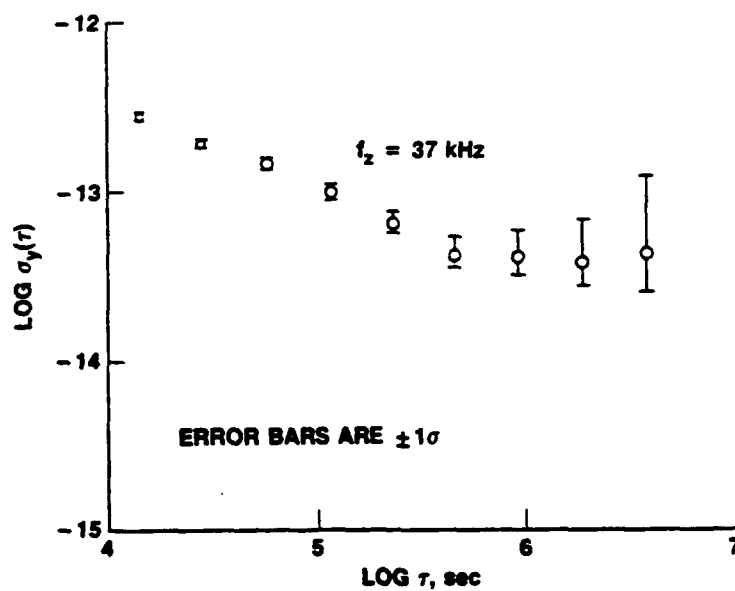


Figure 8. The measured Allan standard deviation of the first Cs Frequency standard at the optimum (power-insensitive) Zeeman frequency setting of 37 kHz. The confidence intervals are 95%. (Data taken by NIST.)

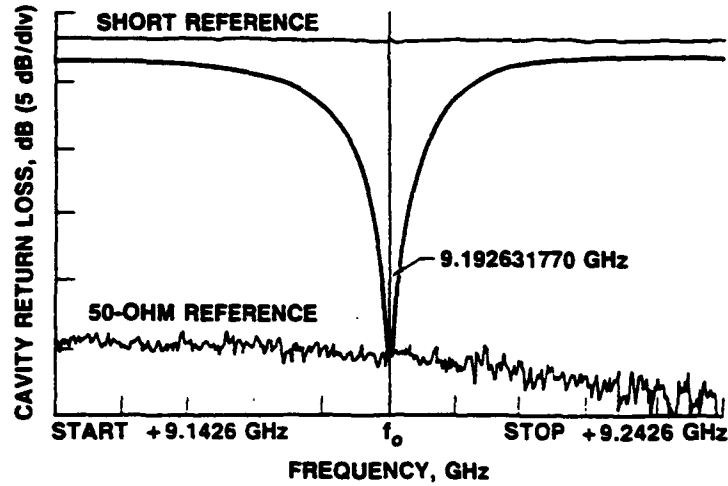


Figure 9. Plot of the microwave cavity return loss of the second Cs frequency standard tuned to a Cs resonance frequency.

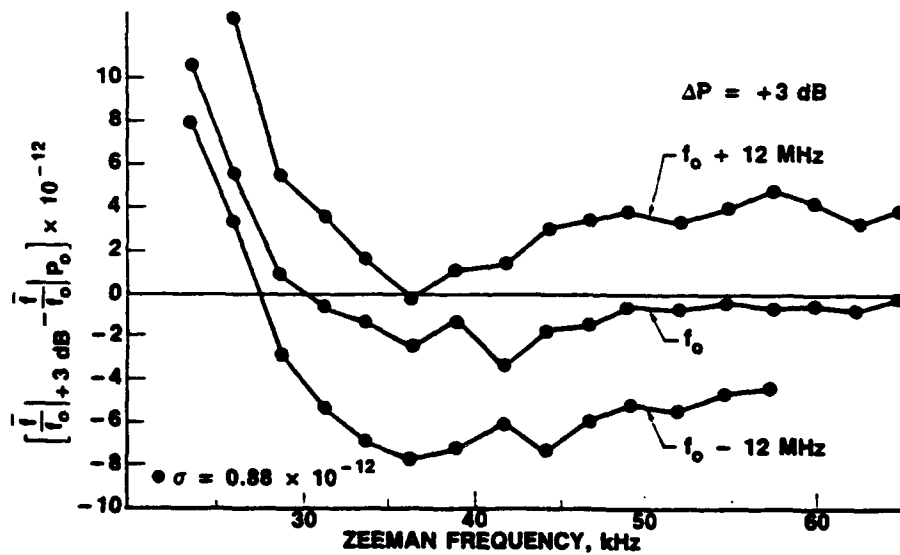


Figure 10. A plot of the difference of the average frequencies as a function of the C-field of the second Cs frequency standard for three microwave-cavity tuned frequencies (f_0 and ± 12 MHz) for a microwave power change of +3 dB above the optimum power level, P_0 .

for changes in microwave power of 3 dB were then measured as a function of the C-field. The cavity was then retuned to 12 MHz above f_0 and the measurements were repeated, after which the cavity was tuned to 12 MHz below f_0 and the measurements were repeated once more. Figure 10 shows the results of the three measurements. This clock is especially interesting because it demonstrated the effect of the cavity pulling. It appears that if the cavity is tuned precisely to f_0 , the Rabi pulling is minimized and there are no clear multiple zero crossings. Also, the slope of the curves is very small for Zeeman frequencies above about 35 kHz. The maximum frequency change was about 3.2×10^{-12} per +3-dB change in microwave power at a Zeeman frequency of about 42 kHz. For this particular Cs clock we can say that, in order to minimize the frequency sensitivity to microwave power variations it may be just as important to tune the microwave cavity properly, perhaps more important than it is to set the C-field at an optimum value.

The third Cs frequency standard measured used a single-beam tube having a different modulation scheme from the first and second Cs frequency standards that we measured. In this third Cs standard we measured the changes in output frequency for a +1 dB microwave power change above P_0 for the cavity tuned at f_0 as well as 40 MHz above and below f_0 . Figure 11 shows the results of the cavity tuning on the C-field curves. We note here that the maximum frequency offset was about 8×10^{-11} per +1-dB power change at a Zeeman frequency of 27 kHz. It is hard to distinguish the effect of cavity pulling, because the Rabi pulling dominates the frequency offset for the +1-dB microwave power change. In this particular frequency standard, we can see clear zero crossings of the C-field curve at about 24, 47, 68, and 83 kHz. The Zeeman frequency difference between adjacent C-field zero crossings of the Rabi-pulling curve is about 23 kHz. The slope at the 47-kHz zero crossing is 0.53×10^{-11} /kHz for a +1-dB microwave power change. Because of this high slope, the long-term frequency stability should improve if one sets the C-field at a zero crossing of the C-field curve. This slope compares to slopes of 0.62×10^{-12} /kHz and 0.11×10^{-12} /kHz for a 1-dB power change for the HP standard and the first standard we measured (see Figures 1 and 6). We caution, however, that this clock was of a very old design, and thus the results presented here should not be considered as typical of that manufacturer's present product.

The fourth Cs frequency standard was sent to us by one of the manufacturers to determine its C-field characteristics; this was a new off-the-shelf production unit. Measurements were made to determine the effect of microwave cavity tuning on the C-field curve for 20 MHz above and below f_0 , as well as at f_0 , for a +3-dB microwave power change above P_0 . Figure 12 shows the plot of the three C-field curves. For the C-field curve tuned at f_0 , the maximum frequency change was about 3.2×10^{-12} at a Zeeman frequency of 39 kHz per 3-dB microwave power change. There were zero crossings at approximately 30, 64, and 74 kHz. The C-field at f_0 had a shape similar to that found earlier on Cs standard number two. The same conclusion can be drawn for this standard as for the second one. The factor perhaps more important than the actual C-field zero crossing is the cavity tuning. The Rabi pulling is minimal in this particular Cs frequency standard. Also, there is no obvious periodicity in the curve, which is in contrast to that found in the HP Cs standard reported on by De Marchi^[1], or in the third Cs standard that we measured (see Fig. 11) earlier. The cavity pulling dominates the frequency changes in this Cs standard.

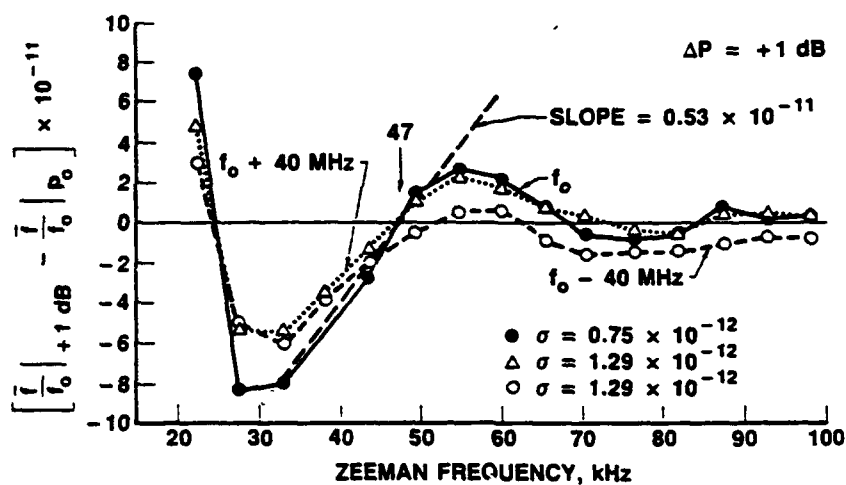


Figure 11. A plot of the difference of the average frequencies as a function of the C-field of the third Cs frequency standard for three microwave-cavity tuned frequencies (f_0 and $\pm 40 \text{ MHz}$) for a microwave power change of +1 dB above the optimum power level, P_0 .

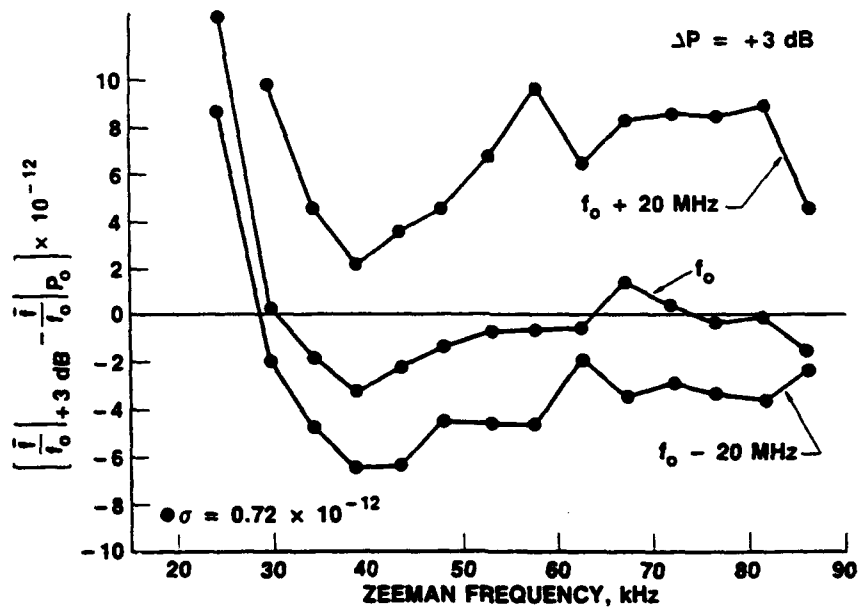


Figure 12. A plot of the difference of the average frequencies as a function of the C-field of the fourth Cs frequency standard for three microwave-cavity tuned frequencies (f_0 and $\pm 20 \text{ MHz}$) for a microwave power change of +3 dB above the optimum power level, P_0 .

INACCURACIES IN THE MEASUREMENT SYSTEM

Our measurement system introduces three sources of error or uncertainty: (1) frequency measurement errors, (2) C-field current setting errors, and (3) power setting errors. The first error (Fig. 6) has been shown to be almost two orders of magnitude below the measurement data. The uncertainty in the C-field current setting is probably on the order of parts in 10^4 in our laboratory environment over the three months during which data were taken; this stability is largely set by the stability of a precision film resistor. The third source of uncertainty, the measurement of the microwave power, is the most difficult of the three to assess. Figure 13 shows the measured power at two levels over 21 days of the C-field measurement time. Over a period of about two weeks, separate stability measurements were made on the power meter and its sensor. It was found that the noise in the measurement system, as measured by the standard deviation, was more than two orders of magnitude below the noise in the power measurements, as shown in Fig. 13. The data in this figure were analyzed statistically and, in conjunction with the data in Fig. 6, were used to calculate the effects of these power variations on the noise floor of the clock.

Using the power data from both power levels in Fig. 13, we computed the Allan standard deviation of the power as a function of time. We then multiplied this statistic by a power sensitivity coefficient to determine the Allan standard deviation of the frequency that would result from these power changes. The power sensitivity coefficient used was $8 \times 10^{13}/\text{dB}$, which was approximately the largest value measured (see Fig. 6).

Table 1 presents the results of this analysis. Column 3 is the Allan standard deviation of the power for time τ , τ being listed in column 1 with the number of data points being listed in column 2. The resulting Allan standard deviation of the clock's frequency is given in column 4 for an assumed $\sqrt{\tau}$ dependency of $3.55 \times 10^{-11}/\sqrt{\tau}$ and a C-field setting resulting in the sensitivity of an $8 \times 10^{-13}/\text{dB}$.

It was concluded from this analysis of the power data (Fig. 13) that, even if the C-field is not set close to an optimum setting, the effect of microwave power changes on the Allan standard deviations will be small for periods of less than a few days. At 2.5 days, the Allan standard frequency deviation that is due to the beam tube noise is still about twice what could result from power variations. Thus, if the Allan standard deviation of the power stayed about constant, the Allan standard frequency deviation due to the beam tube noise and that due to microwave power variations would be about equal at 10 days. Figure 14 is a plot of the data in Table 1.

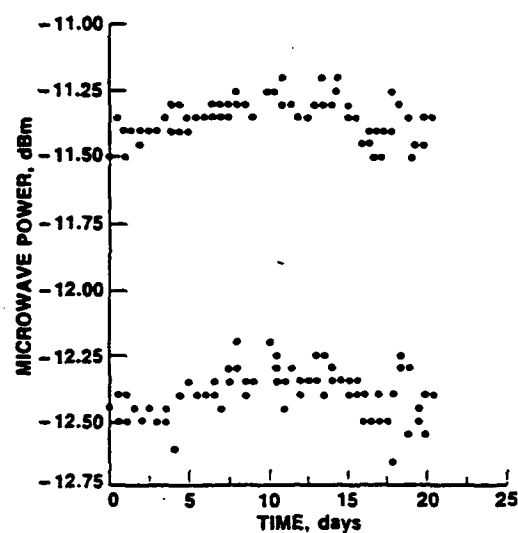


Figure 13. A plot of power measurements made during the C-field experiment. Power was switched between the two nominal levels of -11.35 and -12.35 dBm approximately every 0.4 days.

Table 1. Measurement Data

Time (τ), days		Power Data	Frequency Data	
		Allan Std. Dev. [$\sigma_p(\tau)$], dBm	Allan Std. Dev. [$\sigma_y(\tau) \approx \sigma_p(\tau) \times 8 \times 10^{-13}$]	$\frac{3.55 \times 10^{-11}}{\sqrt{\tau}}$
0.14	128	0.04390	0.3512×10^{-13}	3.228×10^{-13}
0.41	64	0.05794	0.4635×10^{-13}	1.886×10^{-13}
0.82	26	0.03719	0.2975×10^{-13}	1.334×10^{-13}
2.5	12	0.04807	0.3846×10^{-13}	0.7638×10^{-13}

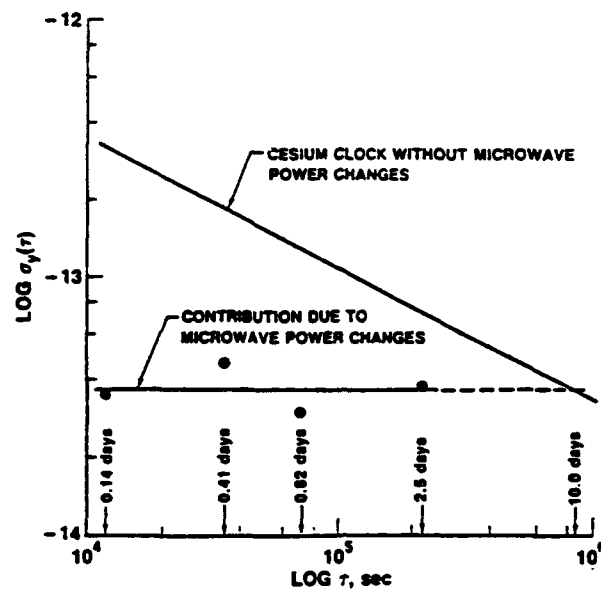


Figure 14. A plot of the calculated contribution of microwave power changes to the Allan standard deviation for Cesium Clock No. 1.

CONCLUSIONS

In this paper, we have presented experimental results of the C-field experiment of De Marchi on four cesium (Cs) frequency standards from two different manufacturers. The results showed that in some Cs frequency standards, there were unique zero crossings that minimized the variations in output frequency caused by changes in microwave power. In one Cs frequency standard, the long-term frequency stability was measured at one of these zero crossings; however, the data did not clearly show a significant stability improvement as had been previously demonstrated on HP Cs standards. None of the other Cs frequency standards clearly had more than one zero crossing, but they all showed that the cavity tuning was effective in minimizing the output frequency variations that were due to power changes. Therefore, to minimize the effects of microwave power changes on output frequency, one should first carefully tune the microwave cavity to the Cs resonance frequency and then set the C-field to a minimum or zero crossing of the C-field tuning curve.

REFERENCES

1. A. De Marchi, "New Insights into Causes and Cures of Frequency Instabilities (Drift and Long-Term Noise) in Cesium Beam Frequency Standards," *Proc. 41st Frequency Control Symposium*, Philadelphia, Pa. (1987), pp. 54-58.
2. A. De Marchi, "Rabi Pulling and Long-Term Stability in Cesium Beam Frequency Standards," *IEEE Trans. Ultrasonics, Ferroelectronics, and Frequency Control* UFFC-34 [6], 598-601 (November 1987).

TECHNOLOGY OPERATIONS

The Aerospace Corporation functions as an "architect-engineer" for national security programs, specializing in advanced military space systems. The Corporation's Technology Operations supports the effective and timely development and operation of national security systems through scientific research and the application of advanced technology. Vital to the success of the Corporation is the technical staff's wide-ranging expertise and its ability to stay abreast of new technological developments and program support issues associated with rapidly evolving space systems. Contributing capabilities are provided by these individual Technology Centers:

Electronics Technology Center: Microelectronics, solid-state device physics, VLSI reliability, compound semiconductors, radiation hardening, data storage technologies, infrared detector devices and testing; electro-optics, quantum electronics, solid-state lasers, optical propagation and communications; cw and pulsed chemical laser development, optical resonators, beam control, atmospheric propagation, and laser effects and countermeasures; atomic frequency standards, applied laser spectroscopy, laser chemistry, laser optoelectronics, phase conjugation and coherent imaging, solar cell physics, battery electrochemistry, battery testing and evaluation.

Mechanics and Materials Technology Center: Evaluation and characterization of new materials: metals, alloys, ceramics, polymers and their composites, and new forms of carbon; development and analysis of thin films and deposition techniques; nondestructive evaluation, component failure analysis and reliability; fracture mechanics and stress corrosion; development and evaluation of hardened components; analysis and evaluation of materials at cryogenic and elevated temperatures; launch vehicle and reentry fluid mechanics, heat transfer and flight dynamics; chemical and electric propulsion; spacecraft structural mechanics, spacecraft survivability and vulnerability assessment; contamination, thermal and structural control; high temperature thermomechanics, gas kinetics and radiation; lubrication and surface phenomena.

Space and Environment Technology Center: Magnetospheric, auroral and cosmic ray physics, wave-particle interactions, magnetospheric plasma waves; atmospheric and ionospheric physics, density and composition of the upper atmosphere, remote sensing using atmospheric radiation; solar physics, infrared astronomy, infrared signature analysis; effects of solar activity, magnetic storms and nuclear explosions on the earth's atmosphere, ionosphere and magnetosphere; effects of electromagnetic and particulate radiations on space systems; space instrumentation; propellant chemistry, chemical dynamics, environmental chemistry, trace detection; atmospheric chemical reactions, atmospheric optics, light scattering, state-specific chemical reactions and radiative signatures of missile plumes, and sensor out-of-field-of-view rejection.